RSC Applied Polymers

ROYAL SOCIETY OF CHEMISTRY

PAPER

View Article Online
View Journal | View Issue

Cite this: *RSC Appl. Polym.*, 2024, **2**, 642

Bio-based electrospun polyamide membrane – sustainable multipurpose filter membranes for microplastic filtration†

Maximilian Rist and Andreas Greiner *

Electrospinning is a highly versatile method for manufacturing filter membranes, contributing to advanced concepts for the production of sustainable membranes for waste water treatment. The use of bio-based polymers could expand the sustainability of such filter membranes significantly. Bio-based PA 6.9, for example, shows great potential for the creation of bio-sourced electrospun filter membranes (EFMs) with high mechanical properties and high resistance to solvents. The polyamide is synthesized from plant oil-based azelaic acid and electrospun from chloroform/formic acid to produce self-standing electrospun nonwovens. These highly porous membranes show high efficiencies of up to 99.8% for the filtration of polystyrene microparticles (PS-MPs) from water. Additionally, the electrospun nonwovens exhibit comparable filtration efficiencies to FFP3 masks for the removal of 0.3 μm particles from air. The membranes show hydrophobic surface behavior (water contact angle of >120°) making them suitable for water oil separation. Efficiencies of up to 99.9% can be achieved for the separation of water and chloroform from 50 vol% mixtures, while maintaining a high permeate flux of up to 5345 L m^{-2} h^{-1}. Additionally, the membranes can be reused for at least ten times without any significant reduction in efficiency or flux.

Received 11th October 2023,
Accepted 2nd January 2024

DOI: 10.1039/d3lp00201b

rsc.li/rscapplpolym

Introduction

Electrospinning is the state-of-the-art method for the production of nonwovens composed of polymer nano- or microfibers.[1] These nonwovens find many different applications including catalysis,[2–4] energy storage[5–7] or filtration.[8–10] Cutting of nonwovens yield short microfibers which can be processed in dispersions. Such dispersions were used for the preparation of sponges or wet-laid membranes.[11,12] Due to their high flexibility, porosity, and specific surface area, electrospun filter membranes (EFMs) often combine high permeability with high rejection rate, making them promising materials for filtration purposes.[13,14] Such EFMs have been successfully used for the filtration of particles from water[8,9,15,16] as well as air[10,17,18] and for the separation of oil and water.[19–23]

Recently, the demand for air filters has seen a sharp increase due to the COVID-19 pandemic.[10] Face masks, in particular, were necessary to prevent spreading of the virus in close quarters. The filters in these face masks must have a high efficiency for the exclusion of particles while having a low pressure drop or high permeability to allow free breathing. The use of electrospun nonwovens as air filtration membranes offers these properties at a lower cost than conventional air filters.[10] In addition, the electrospinning process enables continuous fiber production, which results in very long fibers and prevents them from going airborne.[13] Electrospinning also allows tailoring of the fiber diameter and pore size of the EFM in a wide range reaching three orders of magnitude.[10] Many different polymers have been used to successfully produce EFMs for air filtration, including poly(vinylidene difluoride) (PVDF), polyacrylonitrile (PAN) and polyamides (PA). PA and PAN are especially useful to produce robust filters that need to be used in harsh environments.[24–26] PVDF on the other hand is selected for its hydrophobicity.[27,28] Electrospun membranes for air filtration are usually composites, where the nonwoven is deposited on top of a porous substrate to enhance the generally poor mechanical stability of electrospun nonwovens.[29] On the flipside, self-standing membranes made from only one component can be made in a simpler process, which is more attractive for large-scale production.[10] Additionally, the material can be recycled more easily as the used filter can just be dissolved and the resulting solution used for electrospinning again.[30,31]

While most of the earth is covered by water, only 2.6% of all water on earth is freshwater, and only 0.3% of that is available in liquid form and can be used directly by humans.[9] This

University of Bayreuth, Macromolecular Chemistry and Bavarian Polymer Institute, Universitätsstrasse 30, 95440 Bayreuth, Germany. E-mail: greiner@uni-bayreuth.de

† Electronic supplementary information (ESI) available. See DOI: https://doi.org/10.1039/d3lp00201b

makes drinking water a scarce resource and local availability is often not given. Studies from 2020 show that every fourth human doesn't have access to safe drinking water, and every tenth person lacks even basic water supply.[32] The removal of pollutants from available freshwater is essential for the supply of clean drinking water. Filtration membranes are the choice for the removal of solid particles like microplastics and metal nanoparticles.[33,34] The membranes need to have a high filtration efficiency together with a high water permeability, which is why EFMs are interesting materials for such applications. EFMs for water filtration are commonly prepared from poly(vinyl alcohol) (PVA),[35] PAN,[36] polysulfone (PSF),[37] PVDF,[38] and polyurethane (PU).[39] Self-standing EFMs made of PA have been used for water fiiltration,[40] however, they are mostly applied in composite membranes where they provide the surface hydrophilicity to achieve high water permeability.[41–46]

Another challenging task for the purification of water is the separation of oil from oily wastewater and polluted oceans due to oil spills. The methods currently used are still a challenge.[20,47] Electrospun nonwoven membranes are promising materials for the separation of water and oil. Selective wettability of the EFM can be tailored by choice of material and surface morphology to allow separation of water and oil.[48] EFMs made from poly(vinylidene fluoride-*co*-hexafluoropropylene) (PVDF-HFP) with superhydrophobic surface properties were able to separate oil from water with high efficiency and high flux.[49,50] Similar results were obtained for EFMs made from polylactide (PLA),[51–53] acrylonitrile–butadiene–styrene (ABS)[54] and PA.[55–57] Polyamides can also be used in composite membranes with hydrophobic materials like PVDF to make hydrophilic membranes, where only water is able to penetrate the membrane.[58]

So far, mostly conventional polymers are used for the production of such EFMs, but the availability of bioplastics is growing and their potential application for filtration membranes need to be investigated. PLA-, cellulose- or chitosan-based EFMs are among the most studied bio-based and/or -degradable materials for the production and application of filtration membranes.[59–63] Self-standing membranes made of these materials often lack mechanical stability, making them prone to rupture. Polyamides on the other hand exhibit high mechanical stability due to intermolecular hydrogen bonding. One particularly interesting polyamide is PA 6.9 which is synthesized from bio-based azelaic acid and 1,6-diaminohexane (Scheme 1).[64] The azelaic acid can be sourced from various vegetable and microalgae oils as it is synthesized from common fatty acids like oleic acid. PA 6.9 is structurally similar to PA 6.6, but owing to the extra methylene units in the diacid and the even–odd structure it possesses some unique properties. The PA 6.9 exhibits increased hydrophobicity, resulting in greater dimensional stability, which is advantageous for the production of composites and application in aqueous media.[65] It also has a higher chain flexibility than PA 6.6 because of the greater separation of the amide bonds along the polymer chain.[66] Additionally, production of the bio-based azelaic acid is already commercialized since the 1950s and PA 6.9 is also commercially available.[67]

Herein, we report the preparation of sustainable self-standing EFMs from bio-based PA 6.9. The polyamide was synthesized from hexamethylene diamine and plant oil-based azelaic acid. Nonwovens were prepared by electrospinning from polymer solutions in formic acid/chloroform at different concentrations and cut into membranes. The morphology as well as the surface wettability and the mechanical properties of the prepared membranes were analyzed. The influence of the polymer concentration on the resulting properties was evaluated and discussed. Their potential application as filtration membranes for the filtration of microplastic particles from water and air as well as for the separation of water and oil was investigated. Important filtration properties including flux, permeability, and filtration/separation efficiency were analyzed and compared to existing conventional and bio-based EFMs.

Experimental

Materials

Azelaic acid (technical grade for synthesis), styrene (>99%) and potassium persulfate (99+%) were purchased from Sigma-Aldrich. Hexamethylene diamine (99.5+%) and basic aluminum oxide (5–200 μm, 60A) was purchased from Acros. Chloroform (>99.8%) was purchased from fisher scientific.

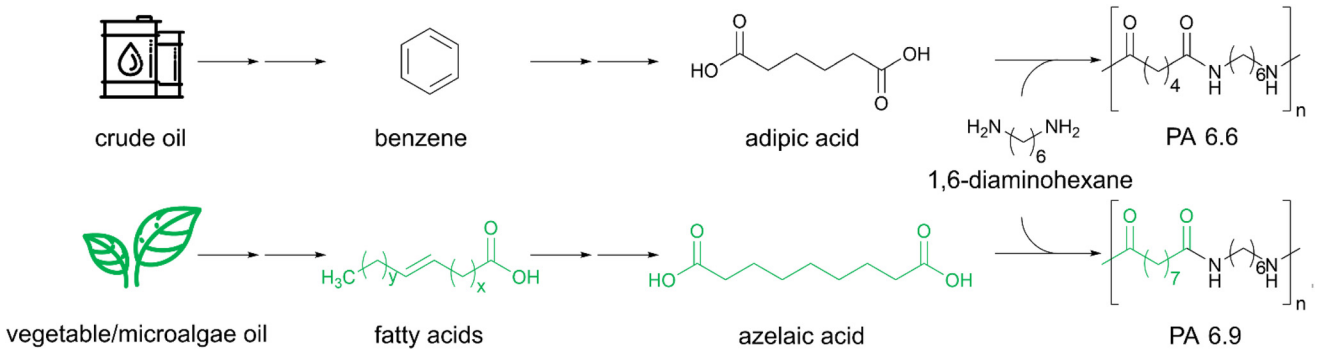

Scheme 1 Synthesis of crude oil-based adipic acid and PA 6.6 in comparison to vegetable/microalgae oil-based azelaic acid and PA 6.9.

Formic acid (99–100%) was purchased from VWR. 1,1,1,3,3,3-Hexafluoro-2-propanol (HFIP, 99%) was purchased from Fluorochem Ltd. Deuterated chloroform ($CDCl_3$, 99.8%) was purchased from Deutero. All solvents for purification were purchased in technical grade from local suppliers.

Purifications

Azelaic acid was recrystallized from ethyl acetate with the addition of activated charcoal. Hexamethylene diamine was distilled and stored under argon atmosphere.

Synthesis of polyamide 6.9

The synthesis of PA 6.9 was adapted from the method used by Tao *et al.*[68] The PA-salt of PA 6.9 was prepared by dissolving equimolar amounts of hexamethylene diamine and azelaic acid in ethanol to form solutions of 10 wt%. Complete dissolution of the diacid was achieved by heating to 40 °C. Upon complete dissolution of the diacid the diamine-solution was added, causing the formation of the PA-salt as a white precipitate. After 1 hour of heating the solution was cooled to 0 °C. The formed PA-salt was recovered by filtration and washed with ethanol to yield the desired PA-salt with a yield of 93%.

For the synthesis of PA 6.9, 400 g of the PA-salt was transferred into a 1 L stainless steel reactor with a mechanical stirrer. Upon exchange of atmosphere with argon to ensure exclusion of oxygen 270 mL of degassed water was added. The resulting slurry was then heated at maximum heating (310 °C jacket temperature) while stirring until a pressure of 15 bar was reached. Then the water steam was slowly removed to keep the reaction running isobar at *ca.* 15 bar, until there was no more water left in the reaction vessel and atmospheric pressure was reached (6 h). Then, the reactor was slowly evacuated over the course of one hour. The polycondensation was proceeded for another three hours at a final melt temperature of 240 °C. Once the torque of the stirrer reached 100 N cm the reaction was stopped by slowly purging with argon until a pressure of 0.2 bar. The polymer was recovered by opening a valve on the bottom of the reaction vessel and quenching of the polymer melt in ice water. The solid polymer was then grinded to receive polymer particles with a maximum diameter of 2 mm. After drying at 70 °C *in vacuo* for 24 h 285 g of PA 6.9 was received as an off-white powder.

Electrospinning of PA 6.9

Polyamide 6.9 was dissolved in 5 mL of a mixture of formic acid and chloroform 1 : 1 v/v (FA/$CHCl_3$) in the specific concentrations. Electrospinning was performed at 24 kV positive voltage for 10 wt% solutions, 25 kV for 12.5 wt% and 26 kV for 15 wt% solutions. The negative voltage was −0.8 kV and the tip to collector distance was 20 cm for all experiments. A rotary disc collector was used as a collector and the flow rate used was 0.4 mL h^{-1} for the 10 and 12.5 wt% solutions and 0.65 mL h^{-1} for the 15 wt% solutions. The total collection time was 1.5 hours for the 10 wt% solutions, 2 hours for the 12.5 wt% and 1 hour for the 15 wt% solutions.

Emulsion polymerization

15.4 g (148 mmol) styrene (destabilized by filtration over basic aluminum oxide) was dispersed in 150 mL of degassed deionized water at 80 °C and a stirrer speed of 200 rpm. A solution of 3.2 mg (0.012 mmol) potassium persulfate in 5 mL degassed deionized water was added quickly. The resulting mixture was stirred over night at 80 °C to form a milky emulsion. The emulsion was filtered over a kitchen sieve to remove larger agglomerated polystyrene particles. The concentration of polystyrene microparticles was determined gravimetrically by taking an aliquot of 5 mL from the dispersion, followed by freeze-drying. The hydrodynamic diameter of the particles was determined *via* dynamic light scattering (DLS) using a PN3704 Zetasizer (Malvern).

Characterizations

Size exclusion chromatography (SEC). The number and weight average molar mass and molar mass distribution of PA 6.9 was measured on a 1200 Infinity (Agilent Technologies/Gynotek) gel permeation chromatography (GPC). The instrument was equipped with a PFG 7 μm precolumn and two main columns (PFG 7 μm 100 Å and PFG 7 μm 300 Å) (PSS, Mainz, Germany). A refractive index detector (RI, Gynotek SE-61) was used for the detection. The sample was dissolved in HFIP (HPLC grade) with potassium trifluoroacetate (8 mg mL^{-1}) and toluene (HPLC grade) as an internal standard in a concentration of 2 mg mL^{-1} and filtered through a 0.22 μm PTFE filter. 20 μL of this solution were injected and measured at a flow rate of 0.5 mL min^{-1} at 23 °C. Calibration of the system was performed with poly(methyl methacrylate) (PSS calibration kit, PSS, Mainz, Germany) in a range of 1720–189 000 Da.

Scanning electron microscopy (SEM). The electrospun membranes were placed onto stups and sputtered with 1.3 nm platinum using a platinum-sputter coater 208HR (Cressington). Recordings were performed with a Leo 1530 (Zeiss) with 3 kV acceleration voltage and at a pressure of 2.0×10^{-5} bar. Images were taken with an inlens and secondary electron detector (Everhart Thornley). A backscattering detector (Centaurus) was used at 10 kV acceleration voltage under the same pressure.

Mechanical properties of membranes. The mechanical properties were determined by uniaxial stress–strain testing on a BT1-FR 0.5TND14 (Zwick/Roell) at room temperature. Test specimens were prepared by cutting out rectangular shaped stripes from the electrospun nonwoven using a scalpel. The dimensions of the test specimens were 5 mm in width with a gauge length of 20 mm. The height of the specimens was measured using a Series 293 (0–25 mm) digital micrometer (Mitutoyo, Neuss, Germany), taking the average of three different positions in the gauge area. The specimens were conditioned for 48 h at room temperature prior to testing. Tensile tests were performed according at 2 mm min^{-1} at a grip to grip separation of 20 mm. The Young's modulus was determined by the slope of the linear region of the stress–strain curves in range of 0.05%–0.25% deformation. At least five specimens were tested for each material and the statistical average is given as a result.

Contact angle measurement. The contact angle measurement for all membranes were performed using a drop shape analyzer (Krüss). For measurement, small rectangular pieces of the nonwovens were cut out and placed on a flat surface. A drop of 4 μL water was produced and placed on top of the membrane and the contact angle was measured after 30 s.

Pore size measurement. Measurement of the pore size distributions were performed using a porometer PSM165 (Topas). Circular-shaped samples (20 mm diameter) were cut out with a scalpel and placed into a measuring adapter with a flow cross-section of 11 mm. For the measurement of the bubble-point, about 5 drops of Topor liquid (surface tension 16.0 mN m^{-1}) was dropped onto the membrane. The used airflow-rate was in the range of 3.6–4200 L h^{-1} and adjusted automatically by the instrument.

Microparticle filtration in water. Circular shaped filters with a diameter of 30 mm were cut out of the membranes using a scalpel. The cut out filters were then placed on a metal mesh and then fixed into a reusable filtering apparatus (Satorius AG), limiting the available filtration area to 3.14 cm^2. The flow rate was adjusted to 1 mL min^{-1} using a LA100 syringe pump (Landgraf Laborsysteme). For each filtration experiment, 45 mL polystyrene microparticle dispersion (300 μg mL^{-1}) were used and the filtrate was collected in intervals of two minutes. The remaining polystyrene concentration in the filtrate was then analyzed *via* UV-Vis to determine the filtration efficiency.

During the experiment, the transmembrane pressure was recorded with a battery powered digital manometer (digi-04) with an accuracy of 0.4% in the range of 0–2.5 bar. The manometer was installed between the syringe pump and the filtering apparatus, and the measured value was noted every minute to calculate the membrane permeability (L m^{-2} h^{-1} bar^{-1}) according to the formula:

$$\text{Permeability} = \frac{V}{A \times \Delta t \times \Delta p}$$

where V is the total volume of the organic phase (L), A is the available area (m^2), Δt is the total filtration time (h) and Δp is the transmembrane pressure (bar).

Quantification of the filtration efficiency. A linear calibration was performed by measurement of the absorption at the absorption maximum of polystyrene (280 nm, Fig. S6†).[69] The polystyrene dispersion was diluted with distilled water to yield five calibration dispersions. The calibration was performed in a range between 1.88 μg mL^{-1} and 30 μg mL^{-1}. The calibration curve is depicted in the ESI,† as well as the absorption spectrum of the polystyrene dispersion.

Aerosol filtration. For the aerosol filtration tests, a Palas MFP 2000 filter test station was used. The test was performed with bis(2-ethylhexyl)sebacate (PALAS DEHS) as a test aerosol. The total volume flow was 8.5 L min^{-1} at a flow velocity of 5 cm s^{-1} and a filter area of 28.3 cm^2. A total number of *ca.* 30 000 particles was measured per filtration test (PALAS aerosol sensor welas® 2100) and at least three filters were tested for each material.

Water–oil separation. For each experiment 4 mL of a mixture of water (colored with methylene blue) and chloroform was used 1 : 1 (v/v). Circular shaped filters with a diameter of 10 mm were cut out of the membranes using a scalpel and placed in a filtration apparatus, limiting the available filtration area to 0.38 cm^2. Each membrane was tested in triplicate and the membranes were reused 10 times. The total time to complete separation of chloroform and water was noted to calculate the flux (L m^{-2} h^{-1}) according to the formula:

$$\text{Flux} = \frac{V}{A \times \Delta t}$$

where V is the total volume of the organic phase (L), A is the available area (m^2) and Δt is the total separation time (h).

Measurement of the water content. A Karl-Fischer titrator 831KF Coulometer (Metrohm) with diaphragm was used to measure the residual water content in the organic phase. Coulomat AG and Coulomat CG were used as anolyte and catholyte for the measurement at 25 °C. Measurements were performed in duplicates and the statistical average is given as the result.

Ultraviolet/visible light spectroscopy (UV-Vis). UV-Vis measurements were performed on a V-630 spectrometer (Jasco) using a quartz cuvette with a measurement depth of 10 mm. The spectrum of the polystyrene-microparticles (PS-MP) was measured in the range of 200–800 nm, with a resolution of 2 nm. Quantitative measurements were performed at the absorption maximum of 280 nm. A calibration was performed in the range of 1.875 ppm to 30 ppm in triplicate. The calibration standards were prepared by dilution of a concentrated PS-MP dispersion with water.

Results and discussion

Evaluation of optimal electrospinning parameters

PA 6.9 was synthesized by melt polycondensation of the PA-salt formed by mixing azelaic acid and hexamethylene diamine in ethanolic solution as previously shown by Tao *et al.*[68] The polymer was drawn out in molten state and grinded to receive granulates with a maximum diameter of 2 mm. SEC measurement of the PA 6.9 confirmed a molecular weight of 34 800 with a dispersity of 2.2, consistent with standard commercial polyamides (Fig. S2†). The PA 6.9 was readily soluble in formic acid/chloroform 1 : 1 (v/v) (FA/$CHCl_3$) with concentrations of up to 20 wt%. The resulting polymer solutions were increasing in viscosity with increasing polymer content. Electrospinning of the final solutions was performed to adjust the parameters for a stable process. It was found, that the viscosity had a great influence on the electrospinning process and no stable jet was formed for the solution with 20 wt% PA 6.9. The growth of stalactite-like structures at the tip of the needle resulting from evaporation of the solvent was observed, which partly blocked the needle. In contrast, the viscosity of the 5 wt% solution was too low and resulted in strong droplet formation. These results are in line with the observations made for the electrospinning

of PA 6.9 from mixtures of formic acid and acetic acid, where solutions between 10 and 20 wt% were spinnable.[66] Finally, steady state electrospinning could be performed for solutions of PA 6.9 with 10, 12.5 and 15 wt% in FA/$CHCl_3$ 1 : 1 (v/v) to form a self-standing membrane. The duration of the electrospinning process of the polymer solutions was adjusted to prepare nonwoven membranes with a comparable thickness in the range of 54–60 μm.

Membrane characterization

The morphology and fiber diameter of the electrospun membranes were analyzed *via* SEM. From the SEM images uniform and smooth fibers can be seen and no formation of beads (Fig. 1). Increasing the polymer concentration also led to an increase of the fiber diameter, which is typical for electrospun polymer fibers. Similar observations were made for electrospun fibers of PA 6.6 from formic acid/chloroform 3 : 1 (v/v)[70] and PA 6.9 from formic acid/acetic acid 1 : 1 (v/v).[66] This might be due to the increased viscosity with increasing polymer concentration, resulting in a lower stretching of the fibers in the Taylor cone. Additionally, a higher polymer concentration also means a lower solvent to polymer ratio. As the solvent evaporates during the electrospinning process, the polymer spends less time in the dissolved state if there is less solvent to begin with, leading again to a lower stretching and thus thicker fibers. Hence, a higher polymer concentration, meaning less solvent per polymer, leads to thicker fibers. Furthermore, the distribution of the fiber diameter is quite narrow for all EFMs made from PA 6.9 with standard deviations of <15%. This shows the great potential of electrospinning for the production of uniform sub-microfibers. Spider net-like structures were observed in all electrospun nonwovens, with a higher prevalence with increasing polymer concentration (Fig. S1†). Similar observations were made in earlier publications for EFMs made from PA 6 and PA 6.6 with increasing polymer concentration.[71] The presence of these structures may be advantageous in terms of filtration performance and they have also been shown to improve the mechanical properties of EFMs.[72]

The mean pore size of the electrospun nonwovens was determined with a capillary flow porometer. Similar to the fiber diameter, the pore size increases with the polymer concentration from 0.55 μm to 1.14 μm (Table 1 and Fig. 2D). The pore structure of electrospun membranes is based on the number of fiber to fiber contacts, as the fibers act as pore boundaries and define the pore.[73,74] The increased viscosity of the polymer solution due to the increased concentration impacts the bending stability of the fibers during solidification between the nozzle and the receiver.[75,76] The resulting change in packing density leads to a lower number of fiber to fiber contacts and ultimately to an increase in pore size.[77] Hence, the pore size of the EFMs prepared from PA 6.9 can be adjusted by the polymer concentration, much like the fiber diameter. Additionally, the pore size distribution was very narrow for all EFMs, which is advantageous for particle filtration (Fig. S3†). Particles having a larger diameter than the pore size will therefore be filtered more easily and with a high

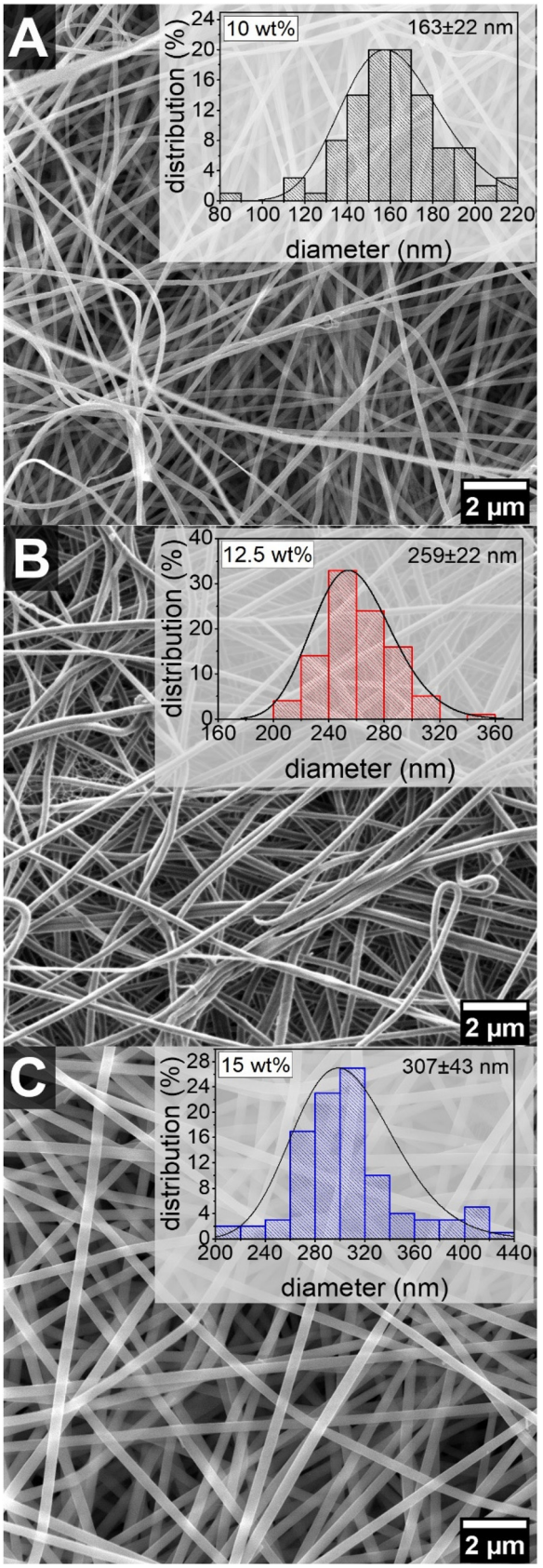

Fig. 1 SEM images and fiber diameter distributions of EFMs prepared from (A) 10 wt%, (B) 12.5 wt% and (C) 15 wt% solutions of PA 6.9 in formic acid/chloroform 1 : 1 v/v.

Table 1 Membrane properties of the PA 6.9 electrospun nonwovens and commercial syringe filter

Material	Thickness [μm]	Average fiber diameter [nm]	Mean pore size [μm]	Areal density [g m^{-2}]	Porosity [%]	Water contact angle [°]
PA 6.9_10 wt%	54 ± 4	163 ± 22	0.55	6.4 ± 0.4	89	132 ± 9
PA 6.9_12.5 wt%	62 ± 2	259 ± 22	0.66	9.7 ± 0.4	85	126 ± 2
PA 6.9_15 wt%	60 ± 3	307 ± 43	1.14	6.8 ± 0.6	90	143 ± 7
PA syringe filter	131 ± 3		0.2			22 ± 2

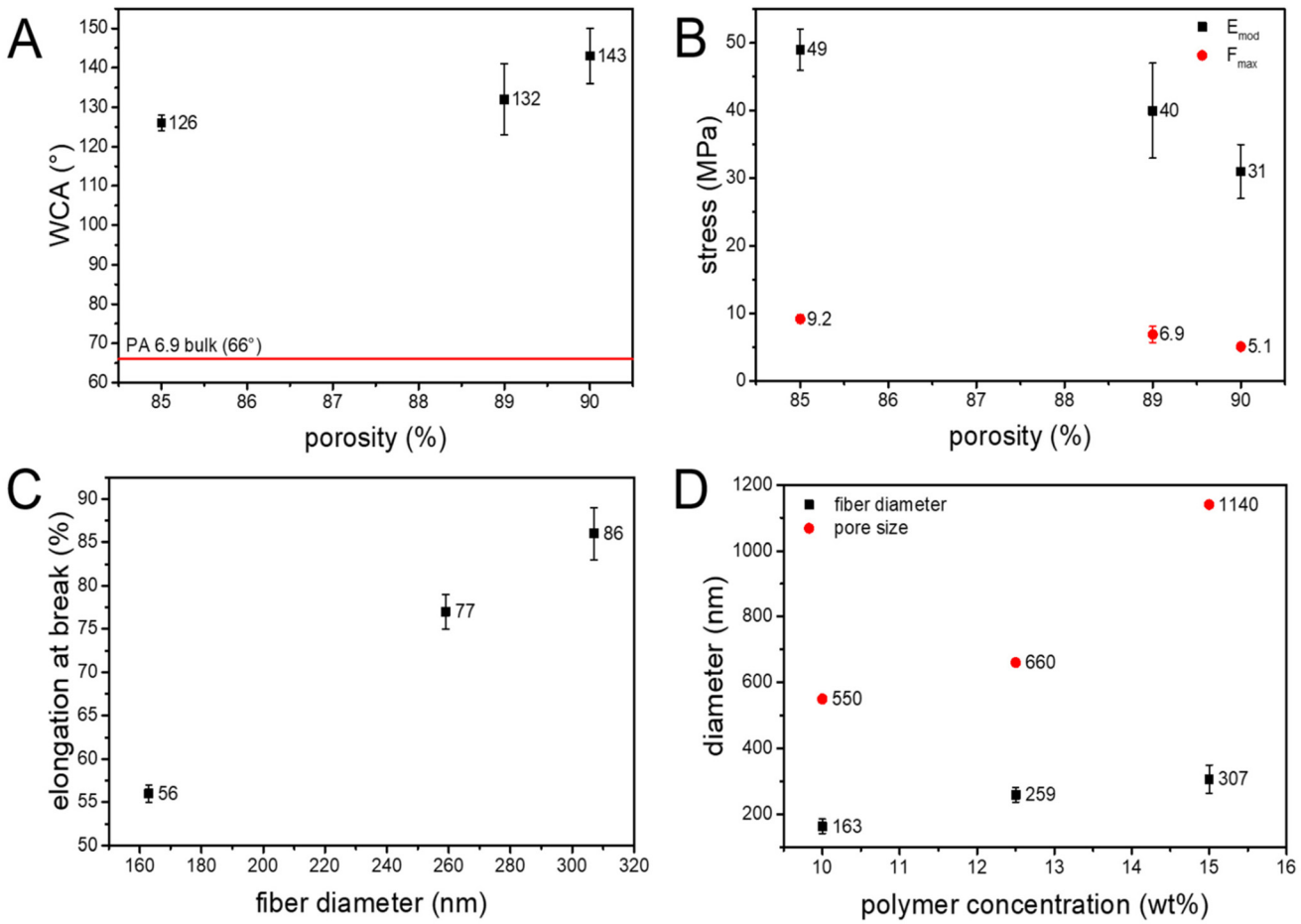

Fig. 2 Different membrane characteristics of the EFMs made from PA 6.9, (A) water contact angle (WCA) and (B) stiffness (E_{mod}) and ultimate tensile strength (F_{max}) in dependence of the porosity, (C) elongation at break against the fiber diameter and (D) fiber diameter and pore size against the polymer concentration.

efficiency. The pore size of the prepared membranes is also in the range of typical microfiltration membranes.[78]

The wettability of electrospun membranes was investigated by measurement of the water contact angle. Interestingly, the electrospun nonwovens showed hydrophobic surface properties with contact angles of >120°. In contrast, PA 6.9 films have a water contact angle of 66°.[79] This is due to the high dependency of the water contact angle on the surface morphology of the electrospun nonwoven. Decreasing the surface roughness of an EFM prepared from PA 6.6 resulted in a 40% lower water contact angle, making the membrane more hydrophilic.[80] The high contact angle and resulting hydrophobic behavior of the EFMs made from PA 6.9 can therefore be explained by their surface roughness. The electrospun nonwovens produced are highly porous structures (>85% porosity) with a high surface roughness.[74] As these pores are typically filled with air (contact angle of 180°), the Cassie–Baxter equation needs to be applied to describe the contact angle of these electrospun membranes.[81,82]

$$\cos\theta = \sigma_1 \times (1 + \cos\theta_1) - 1$$

With θ as the resulting contact angle of the EFM, σ_1 as the solids content of the material and θ_1 as the bulk contact angle of the solid material.

For the EFMs made from PA 6.9 a dependency of the contact angle on the porosity of the membrane could be observed, where an increasing porosity resulted in an increasing contact angle (Table 1 and Fig. 2A). This is further evidence that the Cassie–Baxter model should be applied here, since increasing porosity leads to a lower solids content of the material at the surface of the membrane and thus to an increased hydrophobicity.

The mechanical stability of a filtration membrane is of great importance for its performance. A high mechanical stability prevents the pores from widening due to increased backpressure and ultimately from rupturing during use. Typically EFMs are known to have poor mechanical properties due to their high porosity, random orientation and poor fiber to fiber bonding.[45,83] Several different attempts have been made to improve the mechanical properties of EFMs including UV-cross-linking,[33,34] and solvent vapor treatment.[80] Owing to the generally good mechanical properties of polyamides the EFMs prepared from PA 6.9 showed a much higher tensile strength than membranes prepared from other typical materials like polyvinylidene fluoride (PVDF) and polyacrylonitrile (PAN) (Table 2). Additionally, the results from uniaxial tensile testing of the PA 6.9 membranes are comparable to EFMs made from PA 6.6.[84]

The prepared EFMs showed increasing stiffness (E_{mod}) and tensile strength (F_{max}) with decreasing porosity of the nonwoven (Fig. 2B). Interfiber bond fracture has been proven to be the major damage mechanism for electrospun nonwovens.[85] It was shown, that less interfiber bonds are broken in denser networks, resulting in a higher mechanical stability. Therefore, nonwovens having a lower porosity are stronger and stiffer than ones with a higher porosity.[86,87] Additionally, the nonwovens showed an increasing elongation at break with the fiber diameter (Fig. 2C). This is again in line with observations made for EFMs made from PA 6.6.[70] This could be explained by the also larger pore size leading to a smaller number of loops between the nonwovens, resulting in a longer elongation until the fibers are aligned. Additionally, the thicker fibers could potentially be cold stretched to a greater extent than thinner fibers.

Microplastic particle filtration in water

The filtration performance of the bio-based EFMs for the removal of microplastics from aqueous media was investigated using a dispersion of polystyrene microparticles (PS-MP) in water. Therefore, polystyrene microspheres were prepared by surfactant-free emulsion polymerization in water using the initiator potassium persulfate.[91] The resulting polystyrene spheres had a hydrodynamic diameter of 679 ± 4 nm and formed a stable emulsion in water with a concentration of 300 ppm (Fig. S5†). All three bio-based membranes and the commercial syringe filter were able to remove the PS-MP during filtration with a remarkable efficiency of >99.7%, even after a prolonged filtration time of 45 minutes (Fig. 3A). Comparison with other electrospun membranes reveals that the bio-based EFMs prepared from PA 6.9 show similar performance for the removal of microparticles as EFMs made from conventional materials (Table 3). See Fig. S7† for the experimental setup used for the microplastic particle filtration tests.

There was a large difference in the permeability during microplastic filtration between the EFMs with a pore size of 0.55 μm (PA 6.9_10 wt%) and 0.66 μm (PA 6.9_12.5 wt%). A 0.11 μm larger pore size resulted in a 123% higher initial permeability (Fig. 3B). Further increasing the pore size, on the other hand, did not lead to a significant change of the permeability. Furthermore, only a small decrease of the per-

Table 2 Mechanical properties of EFMs made from PA 6.9 compared to existing materials

Material	F_{max} [MPa]	Elongation at break [%]	E_{mod} [MPa]	Ref.
PA 6.9_10 wt%	6.9 ± 1.2	56 ± 1	40 ± 7	This work
PA 6.9_12.5 wt%	9.2 ± 0.6	77 ± 2	49 ± 3	This work
PA 6.9_15 wt%	5.1 ± 0.4	86 ± 3	31 ± 4	This work
PA 6.6	6.5 ± 0.6	67 ± 11	45 ± 2	84
PVDF	2.8	76	58	88
PAN	4.9	23	—	89
PLA	1.8	200	15	90

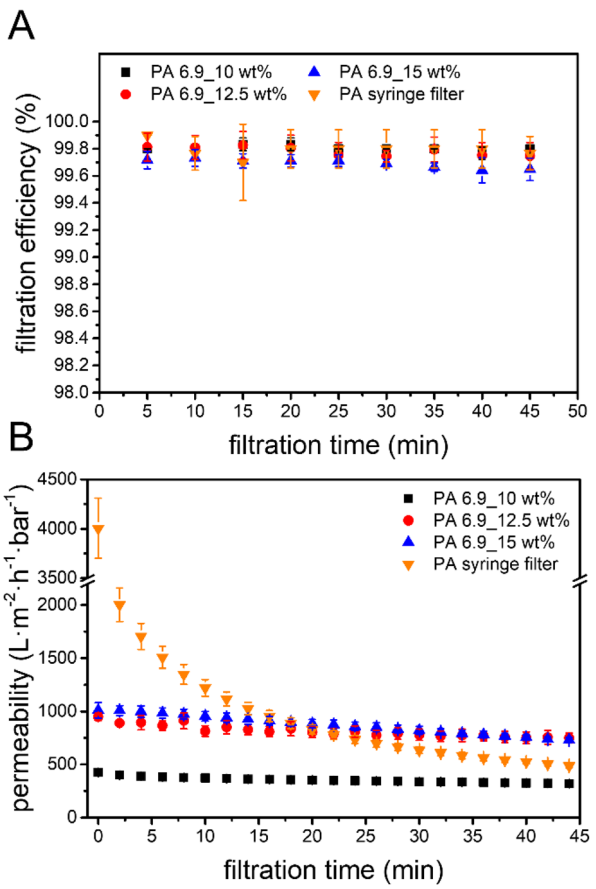

Fig. 3 (A) Filtration efficiency and (B) permeability over time for PS-MP removal using the bio-based EFMs and the PA syringe filter at 1 mL min^{-1}.

Table 3 Filtration performance of different EFMs for the removal of microplastic particles from aqueous media

Material	Membrane thickness [μm]	Particle type and (size) [μm]	Mean pore size [μm]	Filtration efficiency [%]	Initial permeability [L m^{-2} h^{-1} bar^{-1}]	Ref.
PA 6.9_10 wt%	54 ± 4	PS-MP (0.7)	0.55	99.8	424 ± 5	This work
PA 6.9_12.5 wt%	62 ± 2	PS-MP (0.7)	0.66	99.8	949 ± 35	This work
PA 6.9_15 wt%	60 ± 3	PS-MP (0.7)	1.14	99.7	1011 ± 73	This work
PA 6	150 ± 50	PS-MP (1)	0.006	95.9	—	40
PA 6/cellulose	97	PS-MP (0.5)	0.64	>99	570	41
rPET	—	PS-MP (0.5)	0.2	>99	3336 ± 870	92
PAN	*ca.* 70	Unspecified MP (10)	0.15–2	93	22 733	89
PVDF	300	PS-MP (1)	4–11	98	1985	38
PVDF	220	PS-MP (3)	3.59	99.0	45 200	88

meability was observed for all bio-based EFMs during the filtration trials. In contrast, the commercial PA syringe filter showed a much steeper decrease of the permeability, especially in the first 10 minutes. As a result, the performance of the syringe filter became worse than the bio-based EFMs with longer filtration time. After 20 minutes, the bio-based EFMs with a pore size of >0.66 μm showed a higher permeability and therefore better performance. These results indicate a possible application of the bio-based EFMs for the removal of microplastics from aqueous media.

Observation of the membrane cross-section after filtration shows a cake layer of PS microparticles on the top and only a few particles on the bottom side of the membrane (Fig. 4A and Fig. S8†). In the close-up image of the membrane cross section (Fig. 4B and Fig. S8†) some layer separation in the membrane can be observed, allowing a look inside of the membrane. In between the layers, no particles can be observed. This would indicate a surface filtration mechanism which is typical for membranes with smaller or similar pores than the particle size. A surface filtration mechanism would be beneficial in terms of sustainability, as it opens up the possibility of backflushing the membrane in order to reactivate and reuse it. But, these results are only an indication. A closer examination of the inside of the membrane after filtration could provide a better understanding of the filtration mechanism.

Aerosol filtration

The suitability for the removal of aerosols from air was also investigated using the bio-based EFMs from PA 6.9. All three membranes showed excellent efficiency (>99.3%) for the removal of the test aerosol particles down to 0.3 μm (Fig. 5A). With smaller particles the filtration efficiency decreases to 51–83% for 0.2 μm particles. For comparison, FFP3 masks are defined by DIN EN 149 to have a filtration efficiency of >99% for particles sizes down to 0.6 μm. The bio-based EFMs therefore exceed the requirements for these face masks in terms of filtration efficiency. They are more comparable to so-called EPA (efficient particulate air) filters, which are defined by the ISO 29463-1 to have a filtration efficiency of greater 99.5% for particles with a diameter of 0.3 μm.

A good air filtration membrane not only needs to have a high filtration efficiency, but also a low pressure drop. EPA filters should have a maximum pressure drop of 300 Pa and FFP3 masks are not allowed to have a pressure drop of over 500 Pa. In comparison, the prepared EFMs exhibit much higher pressure drops of 2090 ± 286 Pa for PA 6.9_10 wt%, 1710 ± 182 Pa for 12.5 wt% and 2200 ± 381 Pa for 15 wt%, exceeding those limitations. This might be due to the thickness of the membrane, which is known to influence the pressure drop of EFMs.[30] Thinner membranes might still be able to show high filtration efficiency with a reduced pressure drop. Additionally, an increasing trend of the pressure drop with decreasing porosity was observed for the bio-based EFMs (Fig. 5B). This is not surprising, however, since a higher porosity offers less resistance to air flow, a well-known effect in air filtration membranes.[28,93,94] The quality factor is a useful parameter to compare the performance of different filtration membranes, as it combines filtration efficiency and pressure drop. Commercial air filters such as HEPA (high efficiency particulate air), cabin air filters and FFP3 face masks have high quality factors of 15, 10 and 19 kPa^{-1} respectively.[95,96] Compared to these, the bio-based EFMs exhibit lower performance with quality factors ranging between 2.5 and 2.9 kPa^{-1} for particles of 0.3 μm in diameter (Fig. 5B). This is mainly due to the high pressure drop, as the filtration efficiency for all three membranes was >99.3%. Other air filtration EFMs made from PA, PAN or poly(ethylene oxide) (PEO) often have quality factors between 15 and 50 kPa^{-1}, compared to which the bio-based EFMs from PA 6.9 are also inferior.[71]

Water–oil separation

Polyamides generally show a high stability against solvents, making them interesting materials for applications in harsh environments. The EFMs prepared from bio-based PA 6.9 also show hydrophobic surface behavior, making them promising candidates for the separation of water from oil. In order to highlight their potential application, the performance for the separation of chloroform and water in gravity driven filtration was investigated. All three membranes showed excellent separation efficiencies of >99% independent of their pore size and porosity. This is comparable with results obtained for other electrospun, hydrophobic membranes like polyimide (PI) modified with thiolated graphene (GSH/PI) and PVDF-HFP (Table 4). The PVDF-HFP membrane shows a good separation

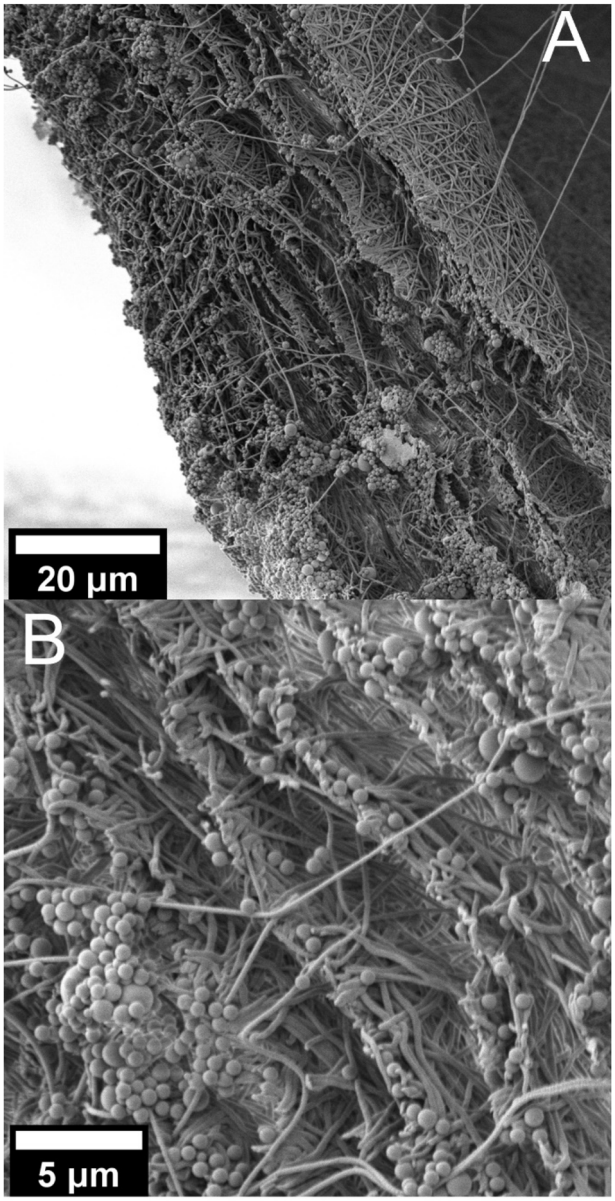

Fig. 4 SEM pictures of the cross section of the PA 6.9_12.5 wt% membrane after filtration, (A) at 1000× magnification and (B) at 3500× magnification.

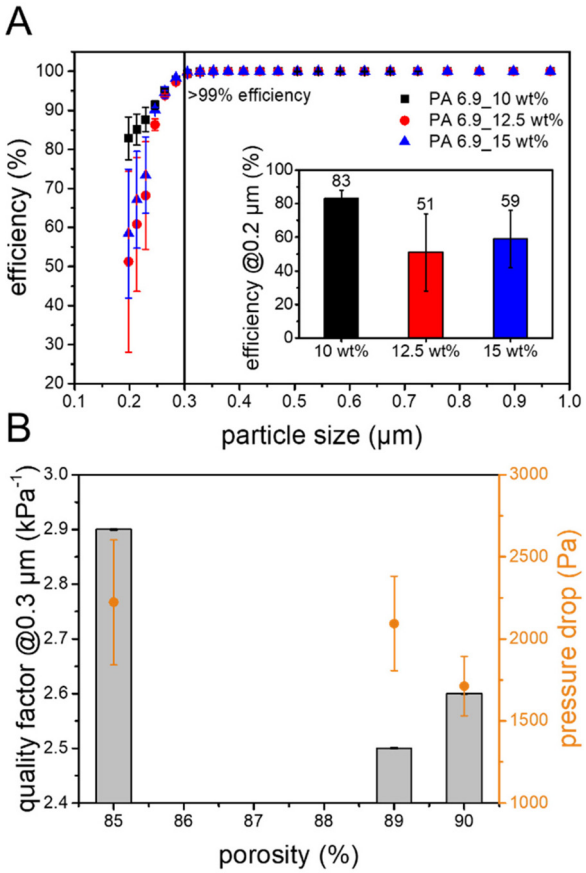

Fig. 5 (A) Particle size dependent filtration efficiency and (B) pressure drop and quality factor against porosity for the aerosol filtration using the bio-based EFMs.

Table 4 Performance of different hydrophobic EFMs for the separation of water and oil

Material	Mean pore size [μm]	Separation efficiency [%]	Initial flux [L m^{-2} h^{-1}]	Ref.
PA 6.9_10 wt%	0.55	99.9 ± 0.0	2878	This work
PA 6.9_12.5 wt%	0.66	99.9 ± 0.1	985	This work
PA 6.9_15 wt%	1.14	99.9 ± 0.0	5345	This work
GSH/PI	—	99.9	2744	97
PVDF-HFP	1.8	99	120	50

efficiency, but at a much lower flux than the membranes prepared from PA 6.9 (120 L m^{-2} h^{-1}).[50] The lower flux could be due to the higher membrane thickness, which is twice that of the PA 6.9 membranes. The modified GSH/PI membranes on the other hand shows a high flux of 2744 L m^{-2} h^{-1} together with an excellent separation efficiency of 99.9%. However, the modification of the electrospun PI membranes to achieve the GSH/PI membranes involves multiple reaction steps. The PA 6.9 membranes on the other hand can be easily produced by electrospinning. Furthermore, they are self-standing membranes without modifications, which facilitates recycling of the membranes considerably. They also combine a high separation efficiency of 99.9% with a high flux ranging from 985 to 5345 L m^{-2} h^{-1}. We observed an increasing permeate flux with the porosity of the membranes. This can be explained by the lower drag acting on the permeate during the flow through the membrane with a higher porosity.

The reusability of the membranes was investigated by repeating the separation tests ten times using the same membrane (Fig. 6). No significant loss in separation efficiency was observed during the cycles. The permeate flux was also very stable during the cycles and only a slight decrease could be observed over ten cycles.

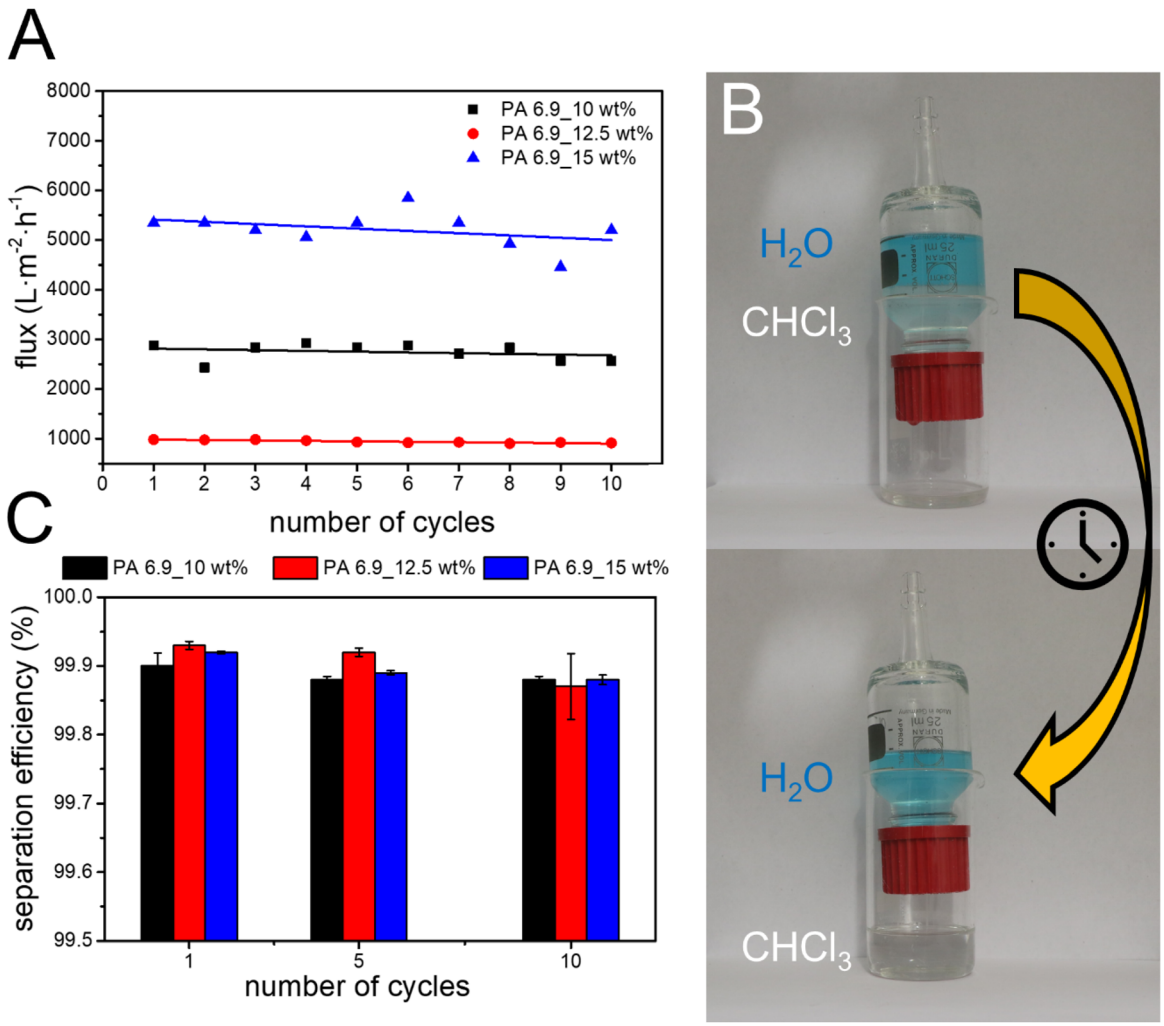

Fig. 6 Results for the separation of water and chloroform, (A) the initial permeate flux for each separation cycle (linear fit), (B) filtration setup with a mixture of chloroform and water before and after filtration, (C) separation efficiency during the first, fifth and tenth cycle.

Conclusions

Bio-based EFMs were prepared by electrospinning from solutions of vegetable oil-sourced PA 6.9 in chloroform/formic acid. Their morphology, as well as their mechanical properties and surface properties were analyzed and tailored by changing the polymer concentration during the electrospinning process. A great influence of the porosity on the mechanical strength and the surface hydrophobicity was observed. The EFMs also showed high efficiency for the removal of microplastic particles from water under prolonged time. Additionally, the membranes showed comparable water permeability to PA composite membranes and better performance than commercial syringe filters. The possible surface filtration mechanism also opens the opportunity of recycling by back-flushing. This highlights the potential of sustainable EFMs prepared from PA 6.9 for the removal of microplastics from polluted water. Furthermore, the membranes were successfully applied for the removal of aerosols from air. The EFMs achieved a filtration efficiency of >99.3% for aerosol particles down to 0.3 μm, the industry standard most penetrating particle size, and up to 83% for 0.2 μm particles. However, the pressure drop of the as-spun membranes was too high for commercial application as air filters. Thinner membranes might be able to achieve similar filtration efficiencies at a lower pressure drop. Due to their high hydrophobicity, the EFMs showed excellent performance for the separation of water and oil with separation efficiencies of 99.9% while maintaining a high permeate flux of up to 5345 L m^{-2} h^{-1}. Reusability of the EFMs for the separation of water and oil was also proven and the membranes could be reused up to 10 times without any significant loss in separation efficiency and permeate flux. In conclusion, this work highlights the potential of PA 6.9 for the production of sustainable filter membranes.

Author contributions

All authors contributed to the manuscript. All authors have given approval to the final version of the manuscript.

Conflicts of interest

There are no conflicts to declare.

Acknowledgements

The authors are indebted for partial financial support to the Federal Ministry of Education and Research (Research project Algae Tex, no. 031b1058B).

This study was cofunded by the Deutsche Forschungsgemeinschaft (DFG, German Research Foundation) – SFB 1357-391977956.

The authors gratefully acknowledge the use of equipment and assistance offered by the Keylab "Small Scale Polymer Processing" and by the Keylab "Electron- and Optical Microscopy" of the Bavarian Polymer Institute at the University of Bayreuth.

References

1 K. D. Patel, H.-W. Kim, J. C. Knowles and A. Poma, Molecularly Imprinted Polymers and Electrospinning: Manufacturing Convergence for Next–Level Applications, *Adv. Funct. Mater.*, 2020, **30**, 2001955.

2 M. O. Pretscher, G. Sitaru, M. Dietel, H. Schmalz, S. Gekle and S. Agarwal, Post-Process-Functionalized Catalytic Electrospun and 2D-Printed Structures for Wolf–Lamb-Type Catalysis, *ACS Appl. Polym. Mater.*, 2021, **3**, 1349–1357.

3 W. Shi, H. Li, R. Zhou, X. Qin, H. Zhang, Y. Su and Q. Du, Preparation and characterization of phosphotungstic acid/PVA nanofiber composite catalytic membranes via electrospinning for biodiesel production, *Fuel*, 2016, **180**, 759–766.

4 E. Formo, E. Lee, D. Campbell and Y. Xia, Functionalization of electrospun TiO2 nanofibers with Pt nanoparticles and nanowires for catalytic applications, *Nano Lett.*, 2008, **8**, 668–672.

5 S. Pazhaniswamy, S. A. Joshi, H. Hou, A. K. Parameswaran and S. Agarwal, Hybrid Polymer Electrolyte Encased Cathode Particles Interface–Based Core–Shell Structure for High–Performance Room Temperature All–Solid–State Batteries, *Adv. Energy Mater.*, 2023, **13**, 2202981.

6 A. Laezza, A. Celeste, M. Curcio, R. Teghil, A. de Bonis, S. Brutti, A. Pepe and B. Bochicchio, Cellulose Nanocrystals as Additives in Electrospun Biocompatible Separators for Aprotic Lithium-Ion Batteries, *ACS Appl. Polym. Mater.*, 2023, **5**, 1453–1463.

7 H. Cai, X. Tong, K. Chen, Y. Shen, J. Wu, Y. Xiang, Z. Wang and J. Li, Electrospun Polyethylene Terephthalate Nonwoven Reinforced Polypropylene Separator: Scalable Synthesis and Its Lithium Ion Battery Performance, *Polymers*, 2018, **10**, 574.

8 A. A. Nayl, A. I. Abd-Elhamid, N. S. Awwad, M. A. Abdelgawad, J. Wu, X. Mo, S. M. Gomha, A. A. Aly and S. Bräse, Review of the Recent Advances in Electrospun Nanofibers Applications in Water Purification, *Polymers*, 2022, **14**, 1594.

9 Z. Uddin, F. Ahmad, T. Ullan, Y. Nawab, S. Ahmad, F. Azam, A. Rasheed and M. S. Zafar, Recent trends in water purification using electrospun nanofibrous membranes, *Int. J. Environ. Sci. Technol.*, 2021, 1–28.

10 I. A. Borojeni, G. Gajewski and R. A. Riahi, Application of Electrospun Nonwoven Fibers in Air Filters, *Fibers*, 2022, **10**, 15.

11 P. Risch and C. Adlhart, A Chitosan Nanofiber Sponge for Oyster-Inspired Filtration of Microplastics, *ACS Appl. Polym. Mater.*, 2021, **3**, 4685–4694.

12 F. Kessel, M. Frieß, O. Hohn, L. Klopsch, C. Zöllner, C. Dirks, M. Scheiffele, F. Vogel and R. Jemmali, Three-dimensional preforming via wet-laid nonwoven technology for ceramic matrix composites, *J. Eur. Ceram. Soc.*, 2023, **43**, 5148–5158.

13 R. Asmatulu and W. S. Khan, in *Synthesis and applications of electrospun nanofibers*, ed. R. Asmatulu and W. S. Khan, Elsevier, Oxford, United Kingdom, 2019, pp. 135–152.

14 G. Nallathambi, D. Baskar and A. K. Selvam, Preparation and characterization of triple layer membrane for water filtration, *Environ. Sci. Pollut. Res.*, 2020, **27**, 29717–29724.

15 X. Xu, Y. Yang, T. Liu and B. Chu, Cost-effective polymer-based membranes for drinking water purification, *Giant*, 2022, **10**, 100099.

16 T. M. Subrahmanya, A. Bin Arshad, P. T. Lin, J. Widakdo, H. K. Makari, H. F. M. Austria, C.-C. Hu, J.-Y. Lai and W.-S. Hung, A review of recent progress in polymeric electrospun nanofiber membranes in addressing safe water global issues, *RSC Adv.*, 2021, **11**, 9638–9663.

17 A. Mamun, T. Blachowicz and L. Sabantina, Electrospun Nanofiber Mats for Filtering Applications-Technology, Structure and Materials, *Polymers*, 2021, **13**, 1368.

18 J. Matulevicius, L. Kliucininkas, T. Prasauskas, D. Buivydiene and D. Martuzevicius, The comparative study of aerosol filtration by electrospun polyamide, polyvinyl acetate, polyacrylonitrile and cellulose acetate nanofiber media, *J. Aerosol Sci.*, 2016, **92**, 27–37.

19 M. Y. Ghadhban, K. T. Rashid, A. A. AbdulRazak and Q. F. Alsalhy, Recent progress and future directions of membranes green polymers for oily wastewater treatment, *Water Sci. Technol.*, 2023, **87**, 57–82.

20 Y. Su, T. Fan, W. Cui, Y. Li, S. Ramakrishna and Y. Long, Advanced Electrospun Nanofibrous Materials for Efficient Oil/Water Separation, *Adv. Fiber Mater.*, 2022, **4**, 938–958.

21 H. M. Mousa, H. S. Fahmy, G. A. M. Ali, H. N. Abdelhamid and M. Ateia, Membranes for Oil/Water Separation: A Review, *Adv Mater. Interfaces*, 2022, **9**, 2200557.

22 J. Zhang, F. Zhang, J. Song, L. Liu, Y. Si, J. Yu and B. Ding, Electrospun flexible nanofibrous membranes for oil/water separation, *J. Mater. Chem. A*, 2019, **7**, 20075–20102.

23 W. Ma, Q. Zhang, D. Hua, R. Xiong, J. Zhao, W. Rao, S. Huang, X. Zhan, F. Chen and C. Huang, Electrospun

fibers for oil–water separation, *RSC Adv.*, 2016, **6**, 12868–12884.
24 R. S. Barhate, C. K. Loong and S. Ramakrishna, Preparation and characterization of nanofibrous filtering media, *J. Membr. Sci.*, 2006, **283**, 209–218.
25 Y. C. Ahn, S. K. Park, G. T. Kim, Y. J. Hwang, C. G. Lee, H. S. Shin and J. K. Lee, Development of high efficiency nanofilters made of nanofibers, *Curr. Appl. Phys.*, 2006, **6**, 1030–1035.
26 C. Liu, P.-C. Hsu, H.-W. Lee, M. Ye, G. Zheng, N. Liu, W. Li and Y. Cui, Transparent air filter for high-efficiency PM2.5 capture, *Nat. Commun.*, 2015, **6**, 6205.
27 X. Wang, H. Xiang, C. Song, D. Zhu, J. Sui, Q. Liu and Y. Long, Highly efficient transparent air filter prepared by collecting-electrode-free bipolar electrospinning apparatus, *J. Hazard. Mater.*, 2020, **385**, 121535.
28 D. Buivydiene, A. M. Todea, C. Asbach, E. Krugly, D. Martuzevicius and L. Kliucininkas, Composite micro/nano fibrous air filter by simultaneous melt and solution electrospinning, *J. Aerosol Sci.*, 2021, **154**, 105754.
29 W. W.-F. Leung, C.-H. Hung and P.-T. Yuen, Effect of face velocity, nanofiber packing density and thickness on filtration performance of filters with nanofibers coated on a substrate, *Sep. Purif. Technol.*, 2010, **71**, 30–37.
30 A. Rajak, D. A. Hapidin, F. Iskandar, M. M. Munir and K. Khairurrijal, Electrospun nanofiber from various source of expanded polystyrene (EPS) waste and their characterization as potential air filter media, *Waste Manage.*, 2020, **103**, 76–86.
31 J. Xue, T. Wu, Y. Dai and Y. Xia, Electrospinning and Electrospun Nanofibers: Methods, Materials, and Applications, *Chem. Rev.*, 2019, **119**, 5298–5415.
32 Change, Environment, Climate and Health, State of the world's drinking water: An urgent call to action to accelerate progress on ensuring safe drinking water for all, *World Health Organization*, 2022.
33 A.-K. Müller, Z.-K. Xu and A. Greiner, Preparation and Performance Assessment of Low-Pressure Affinity Membranes Based on Functionalized, Electrospun Polyacrylates for Gold Nanoparticle Filtration, *ACS Appl. Mater. Interfaces*, 2021, **13**, 15659–15667.
34 A.-K. Müller, Z.-K. Xu and A. Greiner, Sustainable Electrospun Affinity Membranes for Water Remediation by Removing Metal and Metal Oxide Nanoparticles, *ACS Appl. Polym. Mater.*, 2021, **3**, 5739–5748.
35 K. Razmgar and M. Nasiraee, Polyvinyl alcohol –based membranes for filtration of aqueous solutions: A comprehensive review, *Polym. Eng. Sci.*, 2022, **62**, 25–43.
36 S. A. Parekh, R. N. David, K. K. R. Bannuru, L. Krishnaswamy and A. Baji, Electrospun Silver Coated Polyacrylonitrile Membranes for Water Filtration Applications, *Membranes*, 2018, **8**, 59.
37 P. Arribas, M. C. García-Payo, M. Khayet and L. Gil, Heat-treated optimized polysulfone electrospun nanofibrous membranes for high performance wastewater microfiltration, *Sep. Purif. Technol.*, 2019, **226**, 323–336.
38 R. Gopal, S. Kaur, Z. Ma, C. Chan, S. Ramakrishna and T. Matsuura, Electrospun nanofibrous filtration membrane, *J. Membr. Sci.*, 2006, **281**, 581–586.
39 J. Lev, M. Holba, M. Došek, L. Kalhotka, P. Mikula and D. Kimmer, A novel electrospun polyurethane nanofibre membrane—production parameters and suitability for wastewater (WW) treatment, *Water Sci. Technol.*, 2014, **69**, 1496–1501.
40 D. Aussawasathien, C. Teerawattananon and A. Vongachariya, Separation of micron to sub-micron particles from water: Electrospun nylon-6 nanofibrous membranes as pre-filters, *J. Membr. Sci.*, 2008, **315**, 11–19.
41 A. Fauzi, D. A. Hapidin, M. M. Munir, F. Iskandar and K. Khairurrijal, A superhydrophilic bilayer structure of a nylon 6 nanofiber/cellulose membrane and its characterization as potential water filtration media, *RSC Adv.*, 2020, **10**, 17205–17216.
42 F. Yalcinkaya, B. Yalcinkaya and J. Hruza, Electrospun Polyamide-6 Nanofiber Hybrid Membranes for Wastewater Treatment, *Fibers Polym.*, 2019, **20**, 93–99.
43 N. S. Abd Halim, M. D. H. Wirzal, M. R. Bilad, N. A. H. Md Nordin, Z. Adi Putra, A. R. Mohd Yusoff, T. Narkkun and K. Faungnawakij, Electrospun Nylon 6,6/ZIF-8 Nanofiber Membrane for Produced Water Filtration, *Water*, 2019, **11**, 2111.
44 A. R. Jabur, L. K. Abbas and S. A. Moosa, Fabrication of Electrospun Chitosan/Nylon 6 Nanofibrous Membrane toward Metal Ions Removal and Antibacterial Effect, *Adv. Mater. Sci. Eng.*, 2016, **2016**, 1–10.
45 L. Huang and J. R. McCutcheon, Hydrophilic nylon 6,6 nanofibers supported thin film composite membranes for engineered osmosis, *J. Membr. Sci.*, 2014, **457**, 162–169.
46 J.-C. Chen, J.-A. Wu, K.-H. Lin, P.-J. Lin and J.-H. Chen, Preparation of microfiltration membranes with controlled pore sizes by interfacial polymerization on electrospun nanofibrous membranes, *Polym. Eng. Sci.*, 2014, **54**, 430–437.
47 X. Wang, J. Yu, G. Sun and B. Ding, Electrospun nanofibrous materials: a versatile medium for effective oil/water separation, *Mater. Today*, 2016, **19**, 403–414.
48 X. Han and Z. Guo, Graphene and its derivative composite materials with special wettability: Potential application in oil-water separation, *Carbon*, 2021, **172**, 647–681.
49 Z. Liu, B. Gao, X. Huang, H. Ke and J. Xu, Scale-up fabrication of PVDF-HFP nanofibrous membrane with unique surface properties for efficient separation of oil from water, *Text. Res. J.*, 2022, **92**, 1830–1842.
50 L. Zaidouny, M. Abou-Daher, A. R. Tehrani-Bagha, K. Ghali and N. Ghaddar, Electrospun nanofibrous polyvinylidene fluoride–co–hexafluoropropylene membranes for oil–water separation, *J. Appl. Polym. Sci.*, 2020, **137**, 49394.
51 C. Eang, B. Nim, P. Sreearunothai, A. Petchsuk and P. Opaprakasit, Chemical upcycling of polylactide (PLA) and its use in fabricating PLA-based super-hydrophobic and oleophilic electrospun nanofibers for oil absorption and oil/water separation, *New J. Chem.*, 2022, **46**, 14933–14943.

52 Z. Zhou, L. Liu and W. Yuan, A superhydrophobic poly (lactic acid) electrospun nanofibrous membrane surface-functionalized with TiO 2 nanoparticles and methyltrichlorosilane for oil/water separation and dye adsorption, *New J. Chem.*, 2019, **43**, 15823–15831.

53 L. Liu and W. Yuan, A hierarchical functionalized biodegradable PLA electrospun nanofibrous membrane with superhydrophobicity and antibacterial properties for oil/water separation, *New J. Chem.*, 2018, **42**, 17615–17624.

54 S. Jiang, H. Schmalz, S. Agarwal and A. Greiner, Electrospinning of ABS nanofibers and their high filtration performance, *Adv. Fiber Mater.*, 2020, **2**, 34–43.

55 P. Sobolčiak, A. Tanvir, A. Popelka, J. Moffat, K. A. Mahmoud and I. Krupa, The preparation, properties and applications of electrospun co-polyamide 6,12 membranes modified by cellulose nanocrystals, *Mater. Des.*, 2017, **132**, 314–323.

56 P. Zhao, N. Qin, C. L. Ren and J. Z. Wen, Polyamide 6.6 separates oil/water due to its dual underwater oleophobicity/underoil hydrophobicity: Role of 2D and 3D porous structures, *Appl. Surf. Sci.*, 2019, **466**, 282–288.

57 S. Bhagyaraj, P. Sobolčiak, M. A. Al-Ghouti and I. Krupa, Copolyamide-Clay Nanotube Polymer Composite Nanofiber Membranes: Preparation, Characterization and Its Asymmetric Wettability Driven Oil/Water Emulsion Separation towards Sewage Remediation, *Polymers*, 2021, **13**, 3710.

58 R. Lv, M. Yin, W. Zheng, B. Na, B. Wang and H. Liu, Poly (vinylidene fluoride) fibrous membranes doped with polyamide 6 for highly efficient separation of a stable oil/water emulsion, *J. Appl. Polym. Sci.*, 2017, **134**, 44980.

59 V. K. Thakur and S. I. Voicu, Recent advances in cellulose and chitosan based membranes for water purification: A concise review, *Carbohydr. Polym.*, 2016, **146**, 148–165.

60 N. Fiol, Q. Tarrés, M. G. Vásquez, M. A. Pereira, R. T. Mendonça, P. Mutjé and M. Delgado-Aguilar, Comparative assessment of cellulose nanofibers and calcium alginate beads for continuous Cu(II) adsorption in packed columns: the influence of water and surface hydrophobicity, *Cellulose*, 2021, **28**, 4327–4344.

61 H. N. Chang, S. X. Hou, Z. C. Hao and G. H. Cui, Ultrasonic green synthesis of an Ag/CP nanocomposite for enhanced photodegradation effectiveness, *Ultrason. Sonochem.*, 2018, **40**, 1039–1048.

62 R. E. Abou-Zeid, A. Salama, Z. A. Al-Ahmed, N. S. Awwad and M. Youssef, Carboxylated cellulose nanofibers as a novel efficient adsorbent for water purification, *Cellul. Chem. Technol.*, 2020, **54**, 237–245.

63 W. Wang, J. Lin, J. Cheng, Z. Cui, J. Si, Q. Wang, X. Peng and L.-S. Turng, Dual super-amphiphilic modified cellulose acetate nanofiber membranes with highly efficient oil/water separation and excellent antifouling properties, *J. Hazard. Mater.*, 2020, **385**, 121582.

64 A. Todea, C. Deganutti, M. Spennato, F. Asaro, G. Zingone, T. Milizia and L. Gardossi, Azelaic Acid: A Bio-Based Building Block for Biodegradable Polymers, *Polymers*, 2021, **13**, 4091.

65 B. de Schoenmaker, L. van der Schueren, S. de Vrieze, P. Westbroek and K. de Clerck, Wicking properties of various polyamide nanofibrous structures with an optimized method, *J. Appl. Polym. Sci.*, 2011, **120**, 305–310.

66 B. de Schoenmaker, A. Goethals, L. van der Schueren, H. Rahier and K. de Clerck, Polyamide 6.9 nanofibres electrospun under steady state conditions from a solvent/non-solvent solution, *J. Mater. Sci.*, 2012, **47**, 4118–4126.

67 G. C. Goebel, A. C. Brown, H. F. Oehlschlaeger and R. P. Rolfes, *US Pat*, 2813113, 1957.

68 L. Tao, K. Liu, T. Li and R. Xiao, Preparation and properties of biobased polyamides based on 1,9-azelaic acid and different chain length diamines, *Polym. Bull.*, 2020, **77**, 1135–1156.

69 Y. Zhang, T. Paul, J. Brehm, M. Völkl, V. Jérôme, R. Freitag, C. Laforsch and A. Greiner, Role of Residual Monomers in the Manifestation of (Cyto)toxicity by Polystyrene Microplastic Model Particles, *Environ. Sci. Technol.*, 2023, **57**, 9925–9933.

70 M. Afshari, R. Kotek, A. E. Tonelli and D.-W. Jung, in *Nanofibers and Nanotechnology in Textiles*, Elsevier, 2007, pp. 71–89.

71 J. Matulevicius, L. Kliucininkas, D. Martuzevicius, E. Krugly, M. Tichonovas and J. Baltrusaitis, Design and Characterization of Electrospun Polyamide Nanofiber Media for Air Filtration Applications, *J. Nanomater.*, 2014, **2014**, 1–13.

72 N. A. Barakat, M. A. Kanjwal, F. A. Sheikh and H. Y. Kim, Spider-net within the N6, PVA and PU electrospun nanofiber mats using salt addition: Novel strategy in the electrospinning process, *Polymer*, 2009, **50**, 4389–4396.

73 R. Bagherzadeh, S. S. Najar, M. Latifi, M. A. Tehran and L. Kong, A theoretical analysis and prediction of pore size and pore size distribution in electrospun multilayer nanofibrous materials, *J. Biomed. Mater. Res., Part A*, 2013, **101**, 2107–2117.

74 J. H. Wendorff, S. Agarwal and A. Greiner, *Electrospinning. Materials, processing, and applications*, John Wiley & Sons, Weinheim, Hoboken, N.J, 2012.

75 K. P. Feltz, E. A. Growney Kalaf, C. Chen, R. S. Martin and S. A. Sell, A review of electrospinning manipulation techniques to direct fiber deposition and maximize pore size, *Electrospinning*, 2017, **2**, 46–61.

76 C. Mit-uppatham, M. Nithitanakul and P. Supaphol, Ultrafine Electrospun Polyamide-6 Fibers: Effect of Solution Conditions on Morphology and Average Fiber Diameter, *Macromol. Chem. Phys.*, 2004, **205**, 2327–2338.

77 J. L. Lowery, N. Datta and G. C. Rutledge, Effect of fiber diameter, pore size and seeding method on growth of human dermal fibroblasts in electrospun poly(epsilon-caprolactone) fibrous mats, *Biomaterials*, 2010, **31**, 491–504.

78 R. W. Baker, *Membrane technology and applications*, Wiley-Blackwell, Oxford, 3rd edn, 2012.

79 D. I. Richter, *Oberflächencharakterisierung von aliphatischen Polyamiden zur Bewertung adhäsiver Wechselwirkungen in Carbonfaserverbunden*, Berlin, 2004.

80 N. S. Abd Halim, M. D. H. Wirzal, M. R. Bilad, N. A. H. Md Nordin, Z. Adi Putra, N. S. Sambudi and A. R. Mohd Yusoff, Improving Performance of Electrospun Nylon 6,6 Nanofiber Membrane for Produced Water Filtration via Solvent Vapor Treatment, *Polymers*, 2019, **11**, 2117.
81 A. B. D. Cassie and S. Baxter, Wettability of porous surfaces, *Trans. Faraday Soc.*, 1944, **40**, 546.
82 H. Y. Erbil and C. E. Cansoy, Range of applicability of the Wenzel and Cassie-Baxter equations for superhydrophobic surfaces, *Langmuir*, 2009, **25**, 14135–14145.
83 L. Huang, S. S. Manickam and J. R. McCutcheon, Increasing strength of electrospun nanofiber membranes for water filtration using solvent vapor, *J. Membr. Sci.*, 2013, **436**, 213–220.
84 M. M. Mannarino, R. Katsumata and G. C. Rutledge, Structural, mechanical, and tribological properties of electrospun poly(hexamethylene adipamide) fiber mats, *Wear*, 2013, **305**, 58–68.
85 S.-S. Choi, S. G. Lee, C. W. Joo, S. S. Im and S. H. Kim, Formation of interfiber bonding in electrospun poly(etherimide) nanofiber web, *J. Mater. Sci.*, 2004, **39**, 1511–1513.
86 N. Chen, M. K. Koker, S. Uzun and M. N. Silberstein, *In situ* X-ray study of the deformation mechanisms of non-woven polypropylene, *Int. J. Solids Struct.*, 2016, **97–98**, 200–208.
87 N. Chen and M. N. Silberstein, A micromechanics-based damage model for non-woven fiber networks, *Int. J. Solids Struct.*, 2019, **160**, 18–31.
88 M. Li, J. Li, M. Zhou, Y. Xian, Y. Shui, M. Wu and Y. Yao, Super–hydrophilic electrospun PVDF/PVA–blended nanofiber membrane for microfiltration with ultrahigh water flux, *J. Appl. Polym. Sci.*, 2020, **137**, 48416.
89 A. M. Bazargan, M. Keyanpour-rad, F. A. Hesari and M. E. Ganji, A study on the microfiltration behavior of self-supporting electrospun nanofibrous membrane in water using an optical particle counter, *Desalination*, 2011, **265**, 148–152.
90 L. Li, R. Hashaikeh and H. A. Arafat, Development of eco-efficient micro-porous membranes via electrospinning and annealing of poly (lactic acid), *J. Membr. Sci.*, 2013, **436**, 57–67.
91 P. T. Flaviana Yohanala, R. Mulya Dewa, K. Quarta, W. Widiyastuti and S. Winardi, Preparation of Polystyrene Spheres Using Surfactant-Free Emulsion Polymerization, *Mod. Appl. Sci.*, 2015, **9**, 121.
92 N. E. Zander, M. Gillan and D. Sweetser, Recycled PET Nanofibers for Water Filtration Applications, *Materials*, 2016, **9**, 247.
93 N. Wang, Y. Si, N. Wang, G. Sun, M. El-Newehy, S. S. Al-Deyab and B. Ding, Multilevel structured polyacrylonitrile/silica nanofibrous membranes for high-performance air filtration, *Sep. Purif. Technol.*, 2014, **126**, 44–51.
94 Z. Wang, C. Zhao and Z. Pan, Porous bead-on-string poly (lactic acid) fibrous membranes for air filtration, *J. Colloid Interface Sci.*, 2015, **441**, 121–129.
95 H.-J. Kim, D.-I. Choi, S.-K. Sung, S.-H. Lee, S.-J. Kim, J. Kim, B.-S. Han, D.-I. Kim and Y. Kim, Eco-Friendly Poly(Vinyl Alcohol) Nanofiber-Based Air Filter for Effectively Capturing Particulate Matter, *Appl. Sci.*, 2021, **11**, 3831.
96 A. Sharma, H. Omidvarborna and P. Kumar, Efficacy of facemasks in mitigating respiratory exposure to submicron aerosols, *J. Hazard. Mater.*, 2022, **422**, 126783.
97 W. Ma, Y. Li, M. Zhang, S. Gao, J. Cui, C. Huang and G. Fu, Biomimetic Durable Multifunctional Self-Cleaning Nanofibrous Membrane with Outstanding Oil/Water Separation, Photodegradation of Organic Contaminants, and Antibacterial Performances, *ACS Appl. Mater. Interfaces*, 2020, **12**, 34999–35010.